

## REPORT No. 410

### THE THEORY OF WIND-TUNNEL WALL INTERFERENCE

By THEODORE THEODORSEN

#### SUMMARY

*This paper outlines the development of a general theory for the calculation of the effect of the boundaries of the air stream on the flow past an airfoil. An analytical treatment of the conventional closed and open jet types of rectangular wind tunnels disclosed the possibility of devising three distinctly new types: Tunnels with horizontal boundaries only, with vertical boundaries only, and with a bottom boundary only. Formulas are developed for the tunnel wall interference in each case for an airfoil located at the center of the tunnel. The correction is given as a function of the width to height ratio of the tunnel. The formulas are exact for infinitely small airfoils only, but give good approximations for spans up to about three-quarters of the tunnel width.*

*The surprising result is obtained that the three last-mentioned nonconventional types of wind tunnels all are superior to the conventional open or closed tunnels as regards wall interference. It is, indeed, possible to design three distinct types of semiclosed wind tunnels having no wall interference; namely, a square tunnel with horizontal boundaries and no side walls, a rectangular type of a width to height ratio of slightly less than 2:1 and equipped with vertical boundaries only, and one of a ratio of 2:1 and equipped with one horizontal boundary.*

*The author goes on to show that instabilities in the flow may occur for the free jet and the open bottom type tunnels, impairing the predictability of the tunnel wall corrections. A tunnel with a jet free on three sides and restricted only by a lower horizontal boundary extending along the test section from the entrance to the exit cone, is finally recommended as the most promising choice.*

#### INTRODUCTION

The two main factors of concern as regards the application of wind-tunnel data to free-flight conditions are the Reynolds Number and the tunnel wall interference. The finite cross section of the stream of air in a wind tunnel gives rise to a flow past an airfoil or other body which differs distinctly from the flow at "free" air conditions. In the language of mathematics, the solution of the problem of the air flow past the body must satisfy the boundary conditions at the surface of the stream. For tunnels having a closed working section

the solution must be such that the component of the velocity normal to the boundary must be zero. For jet-type wind tunnels the condition to be satisfied at the surface is that of an unaltered or constant flow velocity. Considering a thin layer of air at the outer boundary, this layer will not experience any relative distortion of its individual elements because each element is progressing at a fixed velocity of translation. This statement is, however, only true as regards first order effects. It is, in particular, apparent that the surfaces are distorted in a normal direction. Surface elements originally plane will thus not remain plane.

In the particular types of wind tunnels proposed by the author in the following, both kinds of boundary conditions have to be satisfied simultaneously, inasmuch as the working section is composed of "free" surfaces as well as fixed walls.

It is possible to introduce a third kind of boundary condition; namely, one depicting the condition of a flexible boundary, but this case is solely of mathematical interest.

The construction of the tunnel may be considered as an independent task; the main concern is to produce a flow in the test chamber which is parallel to itself and constant in magnitude. No theoretical reasons exist to preclude the achievement of such an end. Of considerable consequence as regards the operating flow characteristics is the choice of tunnel type and the geometrical shape of its cross section.

A number of cases can fortunately be treated with mathematical stringency. The airfoil is considered to be small compared with the cross section of the tunnel, and is mathematically represented for this purpose by a vortex doublet line through the center of the cross section and extending from the plane of the test section to infinity in the direction of the flow. This simplified assumption yields results which are substantially correct for airfoils extending across as much as three-quarters of the tunnel width. For larger spans the treatment is complicated by the fact that the effect of the interference varies noticeably along the span.

The interference in an open or closed circular tunnel is known from classical hydrodynamics. The effects are numerically identical, but of opposite sign. The closed rectangular tunnel has been treated by Glauert.

(Reference 1.) The present paper is devoted to a systematic analytical treatment of the properties and relative advantages of the several possible arrangements of rectangular tunnels, including the conventional types.

#### WIND-TUNNEL INTERFERENCE

The wind-tunnel wall interference is obtained analytically by arranging a series of vortices in such a manner that the given boundary conditions are satisfied. The problem of the circular cross section is a case of elementary hydrodynamics, and the textbooks will be referred to. Let  $C$  be the cross-sectional area of the tunnel,  $S$  the area of the airfoil, and  $\epsilon$  the upward inclination of the air stream due to the interference at the boundary.

The case of the circle is then given by

$$\epsilon = \pm \frac{1}{8} \frac{S}{C} C_L$$

where the upper sign refers to a closed and the lower sign to an open tunnel. The magnitude  $\epsilon$  is dimensionless and represents an angle of "up-flow." The angle is numerically of some consequence; the ratio  $\frac{S}{C}$  may reach a value of  $\frac{1}{6}$ ,  $C_L$  may reach, say, 1.5, while the

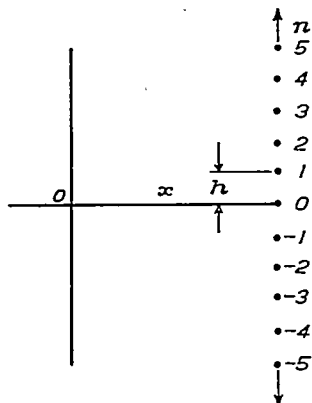


FIGURE 1.—Vertical row of equidistant vortices

constant of proportionality in the most unfavorable case of an open rectangular jet of a 2 : 1 ratio is equal to 0.26. This gives a value of  $\epsilon$  equal to about 3.7°.

Several interesting arrangements of rectangular cross sections will now be treated. For the sake of uniformity in presentation, the case of a closed rectangular section, which is the only type studied in the previous literature, will be included. Consider the following problem. Let  $O$  be the origin of a rectangular system of coordinates. (Fig. 1.) At  $x$  is arranged a vertical column of equidistant line vortices of strength  $\Gamma$  perpendicular to the  $x$ - $y$  plane, the vortices extending from the  $x$ - $y$  plane to infinity in one direction. What is the value of the disturbance at  $x=0$  caused by a vertical column of such vortices extending from  $y=-\infty$  to  $y=+\infty$ ?

If the distance between the vortices be designated  $h$ , we have for the  $n$ th unit above the  $x$ -axis the velocity at the origin perpendicular to the radius vector from that point,

$$v = \frac{\Gamma}{4\pi} \frac{1}{\sqrt{x^2 + n^2 h^2}}$$

and for the vertical component,

$$v_n = \frac{\Gamma}{4\pi} \frac{x}{x^2 + n^2 h^2}$$

The velocity due to all the vortices at  $x$  is parallel to the  $y$ -axis and equal to

$$v_T = \sum_{-\infty}^{+\infty} \frac{\Gamma}{4\pi} \frac{x}{x^2 + n^2 h^2} = \frac{\Gamma}{4\pi} \sum_{-\infty}^{+\infty} \frac{x}{x^2 + n^2 h^2}$$

This expression may be brought into a very simple form:

$$\sum_{-\infty}^{+\infty} \frac{x}{x^2 + n^2 h^2} = \frac{\pi}{h} \sum_{-\infty}^{+\infty} \frac{\frac{\pi x}{h}}{\left(\frac{\pi x}{h}\right)^2 + n^2 \pi^2} = \frac{\pi}{h} \left[ \frac{1}{\frac{\pi x}{h}} + 2 \sum_{n=1}^{\infty} \frac{\frac{\pi x}{h}}{\left(\frac{\pi x}{h}\right)^2 + n^2 \pi^2} \right] = \frac{\pi}{h} \coth \frac{\pi x}{h} \quad (\text{see reference 3, page 135})$$

or

$$\frac{4\pi v_T}{\Gamma} = \frac{\pi}{h} \coth \frac{\pi x}{h} \quad (\text{I})$$

If the vortices are of alternating signs, starting with  $+\Gamma$  at  $y=0$ , a corresponding expression is obtained:

$$\frac{4\pi v_T}{\Gamma} = \frac{\pi}{h} \left[ \frac{1}{\frac{\pi x}{h}} + 2 \sum_{n=1}^{\infty} \frac{(-1)^n \frac{\pi x}{h}}{\left(\frac{\pi x}{h}\right)^2 + n^2 \pi^2} \right] = \frac{\pi}{h} \operatorname{cosech} \frac{\pi x}{h} \quad (\text{II})$$

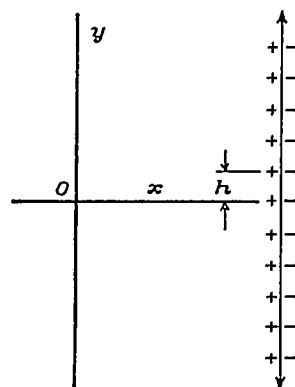


FIGURE 2.—Vertical row of equidistant doublets

The next step is to study the effect of doublets instead of single vortices as in Figure 2. Let the strength of the doublet be  $\Gamma \Delta$ . The doublets, which in the following discussion are termed positive, are so arranged as to correspond to the vortices of an airfoil

at a positive angle of attack and facing the reader; that is, with the air stream down toward the paper.

From the definition of the derivative of  $F(x)$  as

$\lim_{\Delta x \rightarrow 0} \frac{F(x+\Delta x) - F(x)}{\Delta x}$ , it will be seen that the effect of

the doublet is readily obtained as the negative of the derivatives of the expressions already determined, multiplied by  $\Delta L$ .

Hence the flow velocity at 0 in the positive  $y$  direction is, from equation (I),

$$v_x = -\frac{\Gamma \Delta L}{4\pi} \frac{d}{dx} \left[ \frac{\pi}{h} \coth \frac{\pi x}{h} \right] = \frac{\Gamma \Delta L}{4\pi} \left( \frac{\pi}{h} \right)^2 \frac{1}{\sinh^2 \frac{\pi x}{h}} \quad (\text{III})$$

and in the second case, equation (II), with alternating signs

$$v_x = -\frac{\Gamma \Delta L}{4\pi} \frac{d}{dx} \left[ \frac{\pi}{h} \operatorname{cosech} \frac{\pi x}{h} \right] = \frac{\Gamma \Delta L}{4\pi} \left( \frac{\pi}{h} \right)^2 \frac{\cosh \frac{\pi x}{h}}{\sinh^2 \frac{\pi x}{h}} \quad (\text{IV})$$

The effect of a row of doublets arranged along the  $y$ -axis must be treated separately. We are interested in the effect of the row extending from minus to plus infinity minus the unit located at the origin (0, 0). From formula (I) we have for this case with  $x = \Delta x$

$$\frac{4\pi v_x}{\Gamma} = \frac{\pi}{h} \coth \frac{\pi \Delta x}{h} - \frac{1}{\Delta x}$$

where  $\frac{1}{\Delta x}$  is the effect of the doublet at the origin.

This expression may be expanded in a series as follows:

$$\frac{\pi}{h} \left[ \frac{1}{\frac{\pi \Delta x}{h}} + \frac{1}{3} \left( \frac{\pi \Delta x}{h} \right)^2 - \frac{1}{45} \left( \frac{\pi \Delta x}{h} \right)^4 + \dots \right] - \frac{1}{\Delta x} =$$

$$\frac{\pi}{h} \left[ \frac{1}{3} \left( \frac{\pi \Delta x}{h} \right) - \frac{1}{45} \left( \frac{\pi \Delta x}{h} \right)^3 + \dots \right]$$

The negative derivative of this expression times  $\frac{\Gamma \Delta L}{4\pi}$  gives the induced velocity of a series of positive double sources located at  $x=0$  and  $y=nh$  where  $n$  assumes all positive and negative integral values excepting zero. Hence

$$v_x = -\frac{\Gamma \Delta L}{4\pi} \frac{d}{dx} \frac{\pi}{h} \left[ \frac{1}{3} \frac{\pi \Delta x}{h} - \frac{1}{45} \left( \frac{\pi \Delta x}{h} \right)^3 + \dots \right]$$

$$= -\frac{\Gamma \Delta L}{4\pi} \left( \frac{\pi}{h} \right)^2 \left( \frac{1}{3} - \frac{2}{45} \frac{\pi \Delta x}{h} + \dots \right)$$

or for small values of  $\Delta x$

$$v_x = -\frac{1}{3} \left( \frac{\pi}{h} \right)^2 \frac{\Gamma \Delta L}{4\pi} \quad (\text{V})$$

and similarly for a row of doublets on the  $y$ -axis with alternating signs

$$v_x = +\frac{1}{6} \left( \frac{\pi}{h} \right)^2 \frac{\Gamma \Delta L}{4\pi} \quad (\text{VI})$$

By means of the above formulas the interference caused by rectangular tunnels can be determined. The following five cases are investigated:

- I. Tunnel entirely enclosed.
- II. Free jet.
- III. Horizontal boundaries only.
- IV. Vertical boundaries only.
- V. Bottom boundary only.

The wing will be represented by a positive double source, which is equivalent to considering the airfoil small compared with the cross section  $C$  of the tunnel. The conditions for which this assumption is permissible or of value will be specified later.

Case I—Closed tunnel.—The images of the airfoil are conveniently represented by the schematic diagram of Figure 3.<sup>1</sup> Let  $h$  be the height of the tunnel and  $b$

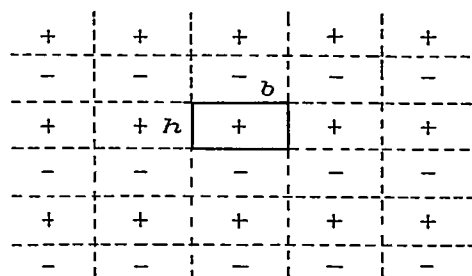


FIGURE 3.—Vortex arrangement for closed tunnel

the width. The upflow velocity caused by a row of doublets located at  $x=mb$  is from (IV) for alternating signs

$$v_x = \frac{\Gamma \Delta L}{4\pi} \left( \frac{\pi}{h} \right)^2 \frac{\cosh \frac{\pi mb}{h}}{\sinh^2 \frac{\pi mb}{h}}$$

For the row at  $x=0$ , from (VI)

$$v_x = \frac{1}{6} \left( \frac{\pi}{h} \right)^2 \frac{\Gamma \Delta L}{4\pi}$$

By summing up the effect of all rows from  $x=-\infty$  to  $x=+\infty$  the total interference effect at the origin is obtained as

$$v_x = \frac{\Gamma \Delta L}{2\pi} \left( \frac{\pi}{h} \right)^2 \left( \frac{1}{12} + \sum_{m=1}^{\infty} \frac{\cosh \frac{\pi mb}{h}}{\sinh^2 \frac{\pi mb}{h}} \right)$$

$$= \frac{\Gamma \Delta L}{2\pi} \left( \frac{\pi}{h} \right)^2 \left( \frac{1}{12} + S_1 \right) \quad (\text{VII})$$

<sup>1</sup> The doublets in Figures 3 to 7 are indicated by single signs.

The series term in the above expression converges rapidly. We have to consider, however, a large number of small terms all of the same sign. A little farther on it will be shown how the value of the expression can be obtained with better than 1 per cent accuracy by the use of an expression representing *all* terms of the series beyond the first.

**Case II—Free jet.**—The images of the airfoil are, for analytical purposes, represented by the schematic

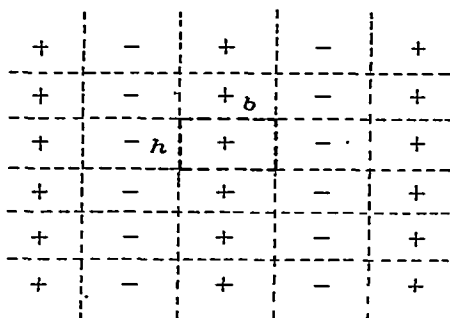


FIGURE 4.—Vortex arrangement for free jet

diagram of Figure 4. For a vertical row located at  $x=mb$  one obtains correspondingly from Formula (III)

$$v_r = \frac{\Gamma \Delta l}{4\pi} \left(\frac{\pi}{h}\right)^2 \frac{1}{\sinh^2 \frac{\pi mb}{h}} (-1)^m$$

where the factor  $(-1)^m$  takes care of the alternating signs of each row. For the row at  $x=0$  from (V)

$$v_r = -\frac{1}{3} \left(\frac{\pi}{h}\right)^2 \frac{\Gamma \Delta l}{4\pi}$$

By summing up for all integral values of  $m$  from minus to plus infinity there results

$$\begin{aligned} v_r &= \frac{\Gamma \Delta l}{2\pi} \left(\frac{\pi}{h}\right)^2 \left[ -\frac{1}{6} + \sum_{m=1}^{\infty} \frac{(-1)^m}{\sinh^2 \frac{\pi mb}{h}} \right] \\ &= \frac{\Gamma \Delta l}{2\pi} \left(\frac{\pi}{h}\right)^2 \left( -\frac{1}{6} + S_2 \right) \end{aligned} \quad (\text{VIII})$$

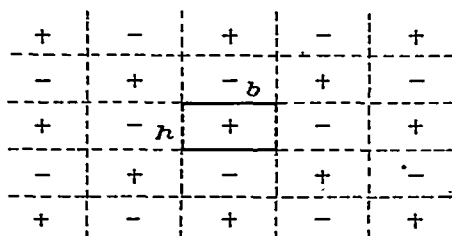


FIGURE 5.—Vortex arrangement for tunnel with horizontal boundaries

**Case III—Top and bottom closed, sides free.**—The arrangement of images is as indicated in Figure 5. The

flow at  $x=0$ , due to an alternating row at  $x=mb$ , is again given by Formula (IV) as

$$v_r = \frac{\Gamma \Delta l}{4\pi} \left(\frac{\pi}{h}\right)^2 \frac{\cosh \frac{\pi mb}{h}}{\sinh^2 \frac{\pi mb}{h}} (-1)^m$$

and for the zero row from Formula (VI) as

$$v_r = \frac{1}{6} \left(\frac{\pi}{h}\right)^2 \frac{\Gamma \Delta l}{4\pi}$$

The total interference is thus given as

$$\begin{aligned} v_r &= \frac{\Gamma \Delta l}{2\pi} \left(\frac{\pi}{h}\right)^2 \left[ \frac{1}{12} + \sum_{m=1}^{\infty} \frac{\cosh \frac{\pi mb}{h}}{\sinh^2 \frac{\pi mb}{h}} (-1)^m \right] \\ &= \frac{\Gamma \Delta l}{2\pi} \left(\frac{\pi}{h}\right)^2 \left( \frac{1}{12} + S_3 \right) \end{aligned} \quad (\text{IX})$$

**Case IV—Sides closed, top and bottom open.**—The arrangement of images is here as indicated in Figure 6

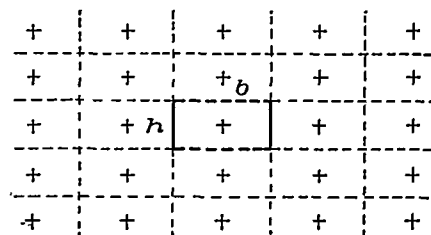


FIGURE 6.—Vortex arrangement for tunnel with vertical boundaries

Notice that all images are positive. The flow at the origin due to a row at  $x=mb$  is from (III)

$$v_r = \frac{\Gamma \Delta l}{4\pi} \left(\frac{\pi}{h}\right)^2 \frac{\cosh \frac{\pi mb}{h}}{\sinh^2 \frac{\pi mb}{h}}$$

except for the row at  $x=0$ , which is given by

$$v_r = -\frac{1}{3} \left(\frac{\pi}{h}\right)^2 \frac{\Gamma \Delta l}{4\pi}$$

Again by summation

$$\begin{aligned} v_r &= \frac{\Gamma \Delta l}{2\pi} \left(\frac{\pi}{h}\right)^2 \left( -\frac{1}{6} + \sum_{m=1}^{\infty} \frac{\cosh \frac{\pi mb}{h}}{\sinh^2 \frac{\pi mb}{h}} \right) \\ &= \frac{\Gamma \Delta l}{2\pi} \left(\frac{\pi}{h}\right)^2 \left( -\frac{1}{6} + S_4 \right) \end{aligned} \quad (\text{X})$$

The labor of summing up the rather slowly converging series  $S_4$  can again be avoided, as will be shown.

**Case V—Bottom or top boundary only.**—The arrangement of images for bottom boundary only is as shown in Figure 7. It may be observed that the

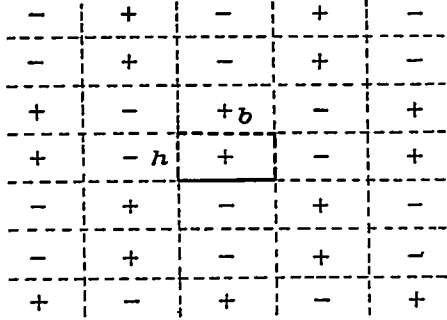


FIGURE 7.—Vortex arrangement for tunnel with bottom boundary only

effects at the origin of the alternate (odd) rows of doublets on either side of the  $x$ -axis cancel in pairs. All odd rows may then be removed, and the distribution of doublets that remains is exactly as that given in Case III and Figure 5, except that  $h$  is replaced by  $2h$ . That is, the induced effects at the origin of a tunnel with bottom boundary only, of width to height ratio  $b/h$ , is equivalent to that of a tunnel with top and bottom boundaries only, of width to height ratio  $b/2h$ . Then

$$v_r = \frac{\Gamma \Delta l}{2\pi} \left( \frac{\pi}{2h} \right)^2 \left[ \frac{1}{12} + \sum_{m=1}^{\infty} \frac{\cosh \frac{\pi m b}{2h} (-1)^m}{\sinh \frac{\pi m b}{2h}} \right] \\ = \frac{\Gamma \Delta l}{2\pi} \left( \frac{\pi}{2h} \right)^2 \left[ \frac{1}{12} + S'_3 \right]$$

where  $S'_3$  is equal to  $S_3$  with each  $h$  replaced by  $2h$ .

The process of evaluating the two rather slowly converging series  $S_1$  and  $S_4$  will now be indicated. The individual terms represent, as shown, the interference due to a row of doublets at  $x = mb$ . For large values of  $m$  it does not matter whether a doublet of strength  $\Gamma \Delta l$  is arranged at  $x = mb$  or whether two vortices of opposite sign and of strength  $\frac{\Gamma \Delta l}{b}$  are substituted at  $x = \left(m - \frac{1}{2}\right)b$  and  $x = \left(m + \frac{1}{2}\right)b$ , respectively.

By the second arrangement all vortices except the one nearest the origin are cancelled by being superimposed on one of opposite sign. The entire effect of all vertical rows of positive doublets extending from  $x = mb$  to infinity is thus represented by the effect of a single positive vortex row of a strength  $\frac{\Gamma \Delta l}{b}$  located at  $x = \left(p + \frac{1}{2}\right)b$  where  $p$  is the number of the last doublet taken into account. The accuracy is the greater, the greater the chosen value of  $p$ . Fortunately, it is found that it is sufficient to make  $p = 1$  and still retain an accuracy of better than 1 per cent. The numerical evaluation of the expressions is thus greatly simplified.

The effect of *single* sources is given by (I) for rows of the same sign as

$$v_r = \frac{\Gamma}{4\pi} \left( \frac{\pi}{h} \right) \coth \frac{\pi x}{h}$$

and by (II) for rows of alternating signs as

$$v_r = \frac{\Gamma}{4\pi} \left( \frac{\pi}{h} \right) \operatorname{cosech} \frac{\pi x}{h}$$

The series  $S_1 = \sum_{m=1}^{\infty} \frac{\cosh \frac{\pi m b}{h}}{\sinh^2 \frac{\pi m b}{h}}$  may then accordingly

$$\text{be written as } S_1 = \sum_{m=1}^{\infty} \frac{\cosh \frac{\pi m b}{h}}{\sinh^2 \frac{\pi m b}{h}} \\ + \frac{1}{b} \left( \frac{\pi}{h} \right)^{-1} \operatorname{cosech} \frac{\pi \left( p + \frac{1}{2} \right) b}{h}$$

and  $S_4 = \sum_{m=1}^{\infty} \frac{1}{\sinh^2 \frac{\pi m b}{h}}$  may be written as

$$S_4 = \sum_{m=1}^{\infty} \frac{1}{\sinh^2 \frac{\pi m b}{h}} + \frac{1}{b} \left( \frac{\pi}{h} \right)^{-1} \coth \frac{\pi \left( p + \frac{1}{2} \right) b}{h}$$

As mentioned above, we obtain accuracy greater than is needed for any practical purposes by making  $p = 1$  in the above finite series expression. The remaining series  $S_2$  and  $S_3$  are obtained without any difficulties.

The expressions (VII) to (X) giving the induced flow at  $x = 0$  are all of the form

$$v_r = \frac{\Gamma \Delta l}{2\pi} \left( \frac{\pi}{h} \right)^2 (a + \Sigma)$$

where  $\Sigma$  stands for  $S_1, S_2, S_3$ , or  $S_4$ , and  $a$  is a numerical constant. By means of the aerodynamical relation

$$\Gamma \Delta l \rho V = \frac{1}{2} C_L \rho V^2 S$$

where  $\rho$  is the density and  $V$  the velocity of the medium, and by putting

$$\frac{v_r}{V} = \epsilon,$$

the upward inclination of the air stream, there results

$$\epsilon = \frac{C_L S}{4\pi} \left( \frac{\pi}{h} \right)^2 (a + \Sigma)$$

or with  $bh = C$  and  $\frac{b}{h} = r$

$$\epsilon = \frac{C_L S \pi r}{C} (a + \Sigma)_\pi$$

On writing

$$\epsilon = \frac{C_L S}{C} \delta \quad (\text{XII})$$

where

$$\delta = \frac{\pi r}{4} (a + \Sigma) \quad (\text{XIII})$$

it is noticed that the angle of up-flow  $\epsilon$  is proportional to the lift coefficient  $C_L$ , to the ratio of wing area to tunnel cross section  $\frac{S}{C_p}$  and to the quantity  $\delta$  which in turn is seen to be a function solely of the width to height ratio  $\frac{b}{h}$  or  $r$ .

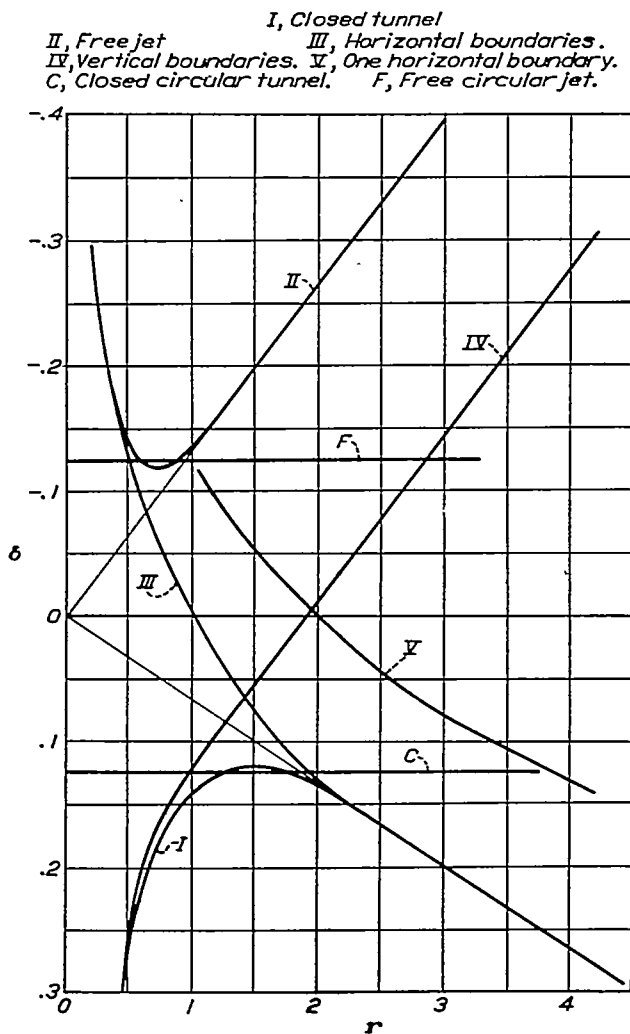


FIGURE 8.—Tunnel-wall correction  $\delta$  for five types of rectangular tunnels of width-height ratio  $r$

The values of  $\delta$  for the five cases considered are given below:

$$\begin{aligned} \text{I. } \delta &= \frac{\pi r}{4} \left( \frac{1}{12} + S_1 \right) \\ \text{II. } \delta &= \frac{\pi r}{4} \left( -\frac{1}{6} + S_2 \right) \\ \text{III. } \delta &= \frac{\pi r}{4} \left( \frac{1}{12} + S_3 \right) \\ \text{IV. } \delta &= \frac{\pi r}{4} \left( -\frac{1}{6} + S_4 \right) \\ \text{V. } \delta &= \frac{\pi \cdot r}{4 \cdot 2} \left( \frac{1}{12} + S'_3 \right) \end{aligned}$$

These values are given in Table I and also plotted in Figure 8 against the single variable  $r$  as abscissa. This figure gives in a convenient way the essential results of the preceding analysis.

The square tunnel,  $\frac{b}{h}=1$ , gives identical numerical values of the interference whether it is open or closed, as is also the case for the circle. The square tunnel with horizontal boundaries shows no interference. A rather interesting result! Notice also that the open tunnels of the conventional width to height ratio exhibit a much larger correction factor than the closed type. Notice further that all of the proposed types are superior to the conventional ones and in particular the surprisingly beneficial effect of a lower horizontal boundary on an otherwise free jet.

#### WIND TUNNELS FREE FROM WALL INTERFERENCE

Inasmuch as wind-tunnel testing is largely concerned with the prediction of free-flight performance of aircraft, it is highly desirable to employ a wind tunnel having no wall interference. Such a tunnel is in this respect entirely equivalent to an air stream of infinite cross section.

The results of the preceding analysis as represented in Figure 8 show that we are perfectly able to devise such a tunnel. Curve III, which corresponds to Case III, crosses the  $\delta=0$  line at  $r=1$ , showing that a square tunnel with walls at top and bottom and both sides removed has zero wall interference. Such a type of tunnel exhibits the particular advantages of the open-jet tunnel and is distinctly superior to both of the conventional types by reason of the fact that it has zero wall interference, or stated otherwise, that it is equivalent to an infinite jet of air.

It is further noticed that the curve IV representing the tunnel with closed sides crosses the  $\delta=0$  line at  $r=1.9$ , showing that a rectangular jet of a width to height ratio of a little less than 2:1 and equipped only with vertical walls exhibits zero wall interference. There is, however, a condition which renders the use of a tunnel wall correction in this particular case rather questionable.

A single fixed horizontal boundary has also a surprisingly beneficial guiding effect. The interference for the case of a 2:1 tunnel is identical with that of the square tunnel of Case III and is zero. Curve V represents a tunnel equipped with a bottom boundary only. The interference is small compared with the free jet type. Whether a fixed bottom or top boundary is employed is immaterial, since the result of the analysis in both cases is the same. As regards the accurate prediction of the interference effect, it will be pointed out, however, that it is necessary to employ a tunnel with a fixed bottom.

## EFFECT OF THE EXIT CONE

The preceding Case II refers strictly to a *free jet*. As such is defined a jet which meets no obstructions behind the model body. Correspondingly, in Case IV there must be no obstruction to prevent the free flow of the air in a vertical direction.

The main effect of the exit cone as regards the wall interference is to guide the air back into its original direction. In a well-designed cone with a small angle of divergence and sufficient bell we may assume this end to be achieved completely, as indicated in Figure 9.

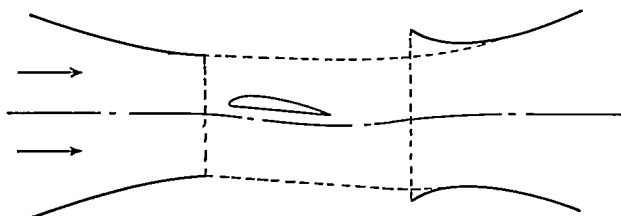


FIGURE 9.—Showing guiding effect of exit cone

The effect of the cone may then, as far as the interference goes, be equivalent to the creation of a counter-circulation of magnitude  $-\Gamma$  located some distance behind the entrance of the cone. The "trailing" vortices will thus not extend from the plane of the airfoil to infinity, as was assumed in the earlier cases, but will close themselves in the exit cone. The numerical value of the interference can readily be found in each particular case, although the method is rather cumbersome.

The solution is mathematically obtainable; there exist, however, some practical difficulties concerning the assumption of the type of flow to be expected in the exit cone. If the cone is rather large and of poor efficiency, a condition similar to Case II, that of an entirely free jet, may actually occur. When the downflow becomes large, the possibility exists that the jet may break loose from the upper side of the cone and follow along the lower. Not only that, but, if the exit cone has an entrance too slightly belled or with no bell at all, the air may *spill* underneath the exit cone. It is entirely possible to imagine that the jet is deflected downward to such an extent that the correction will exceed that of a free jet. The difficulty in these several cases is that the correction factor  $\delta$  is dependent on the amount of the downflow and on factors of rather vaguely definable and unstable nature. In fact, it is probable that the interference is not even a continuous function of the downflow, but is subject to abrupt changes at certain critical values.

If the tunnel is closed entirely or on the top and bottom sides, this difficulty is dispensed with and the exact mathematical prediction of the tunnel wall correction is possible. This fact is essential, since there exists no experimental method by which the existing angle of downflow of the air current at the location of the test model can be obtained.

Attention is, therefore, again directed to the tunnels which have already been referred to as having no wall interference. One of these is of a square cross section with two horizontal fixed boundaries. In contrast to the second type of tunnel with no wall interference, there is in this case no possibility of spillage. The lateral deflection of the air stream is negligible, compared with the vertical, and since the air stream enters the diffuser cone in perfect alignment no radical changes in the type of flow in the cone are to be expected. The third type of the proposed tunnels, the one with a lower boundary only, will obviously achieve the same end. Because a more efficient utilization of the cross section of this tunnel is possible, and since the interference for a 2:1 tunnel is eight times smaller than that for the free jet type of the same side ratio, the superiority of this latter type is obvious.

## EFFECT OF LARGE WING SPAN

The effect of the airfoil has hitherto been represented by vortex doublets. The permissibility of this purely mathematical simplification will now be given some attention. Let us consider the airfoil to be represented by a vortex pair located a distance apart comparable to the width of the tunnel.

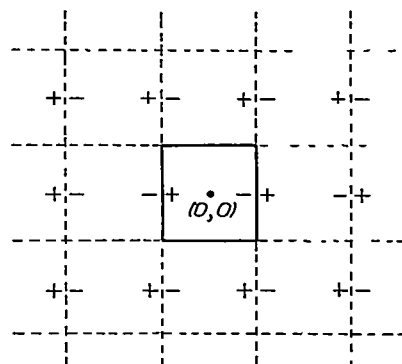


FIGURE 10.—Vortex arrangement in closed square tunnel with airfoil span three-fourths tunnel width

Let Figure 10 represent a closed tunnel. For single alternating vortices in a vertical row, Equation (II) gives

$$\frac{4\pi v_n}{\Gamma} = \frac{\pi}{h} \operatorname{cosech} \frac{\pi x}{h}$$

But

$$\Gamma \cdot \Delta l_p V = \frac{1}{2} \rho V^2 S C_L$$

Hence

$$\epsilon = \frac{v_n}{V} = \frac{S C_L}{8 \Delta l h} \operatorname{cosech} \frac{\pi x}{h} \quad (\text{XIV})$$

For the *first* row on either side of the origin, however, it is necessary to omit the vortex located on the  $x$ -axis, or

$$\epsilon = \frac{S C_L}{8 \Delta l h} \left( \operatorname{cosech} \frac{\pi x}{h} - \frac{1}{\pi x} \right) \quad (\text{XV})$$

These formulas will be applied to the square tunnel with  $\Delta l = \frac{3}{4}b$  or the span of the airfoil equal to three-quarters of the tunnel width. The interference at the center ( $x=0$ ) is

$$\delta = \frac{1}{3} \left( -\frac{1}{\sinh \frac{3}{8}\pi} + \frac{1}{\frac{3}{8}\pi} + \frac{1}{\sinh \frac{5}{8}\pi} - \frac{1}{\sinh \frac{11}{8}\pi} + \frac{1}{\sinh \frac{13}{8}\pi} + \dots \right) = 0.147$$

and the interference at the tip

$$\delta = \frac{1}{6} \left( -\frac{1}{\sinh \frac{3}{4}\pi} + \frac{1}{\frac{3}{4}\pi} + \frac{1}{\sinh \frac{1}{4}\pi} - \frac{1}{\sinh \pi} + \frac{1}{\sinh \frac{5}{4}\pi} + \frac{1}{\sinh \pi} - \frac{1}{\sinh \frac{7}{4}\pi} + \dots \right) = 0.239$$

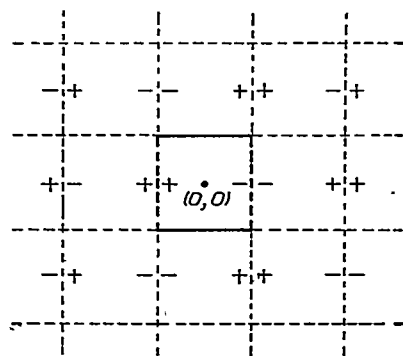


FIGURE 11.—Vortex arrangement in square tunnel with horizontal boundaries with airfoil span three-fourths tunnel width

The next important case, III, horizontal boundaries only, is shown in Figure 11. At the center

$$\delta = \frac{1}{3} \left( -\frac{1}{\sinh \frac{3}{8}\pi} + \frac{1}{\frac{3}{8}\pi} - \frac{1}{\sinh \frac{5}{8}\pi} + \frac{1}{\sinh \frac{11}{8}\pi} + \dots \right) = -0.028$$

At the tip

$$\delta = \frac{1}{6} \left( -\frac{1}{\sinh \frac{3}{4}\pi} + \frac{1}{\frac{3}{4}\pi} - \frac{1}{\sinh \frac{1}{4}\pi} + \frac{1}{\sinh \pi} + \frac{1}{\sinh \frac{5}{4}\pi} - \frac{1}{\sinh \pi} + \frac{1}{\sinh \frac{7}{4}\pi} + \dots \right) = -0.148$$

This calculation can be easily performed for any particular case by means of the formulas (XIV) and (XV). It is left to the reader, therefore, to check any case with which he is concerned. Notice from the preceding examples that it is undesirable to use an airfoil

which has an equivalent span of three-quarters of the width of a square tunnel because the interference differs too much over the span. The flow at the center does not, however, differ materially from the flow at shorter spans. It is thus possible to study the flow near the fuselage of an airplane or model which may otherwise be too large for the tunnel.

#### WING INTERCEPTING THE TEST TUNNEL

The undesirable condition of unequal interference along the span is still more pronounced when the wing span exceeds the width of the tunnel. In the limiting case, let the circulation along the wing be constant. The trailing vortices are then, mathematically speaking, located at  $x = \pm \frac{b}{2}$ . Considering the case of a closed tunnel, we can readily see that the real and a corresponding pair of virtual vortices cancel each other and that all the remaining virtual vortices cancel each other in pairs. On the other hand, for a free jet the interference near the vertical surface approaches theoretically an infinite value due to the nearness of the first image. The flow near the center, however, remains finite.

It is difficult to imagine that tests on airfoils intercepting a free test jet would be of any value whatsoever except in the study of local conditions. The prediction of the lift distribution is mathematically of great difficulty, and moreover, the distribution differs too greatly along the span to permit the application of the results to other conditions. It may be postulated that the interference effect along the span must be nearly a constant. Only in this case can a correction be applied that is of sufficient simplicity and accuracy.

#### CONCLUSIONS

Several rectangular wind tunnel arrangements that exhibit zero or negligible wall interference have been brought out by a mathematical analysis of the general problem of tunnel interference. Uniform formulas have been presented for the calculation of the wall interference for the conventional as well as for the newly proposed wind tunnels.

It has been indicated that the exact prediction of the interference for tunnels with no lower horizontal boundaries is greatly impaired by the inherent instability of the flow in the exit cone. Attention has been brought to the importance of employing an exit cone with a small angle of divergence, and also to the importance of having the air stream properly centered at the entrance of the jet. A tunnel with a jet free on three sides and restricted only by a lower horizontal boundary extending along the test section from the entrance to the exit cone, is finally recommended as the most promising choice. The correction for this type is from



five to eight times smaller than that of the corresponding free jet type.

LANGLEY MEMORIAL AERONAUTICAL LABORATORY,  
NATIONAL ADVISORY COMMITTEE FOR AERONAUTICS,  
LANGLEY FIELD, VA., *October 9, 1931.*

## REFERENCES

1. Glauert, H.: The Elements of Aerofoil and Airscrew Theory. Cambridge University Press, 1926.
2. Prandtl, L., and Betz, A.: Vier Abhandlungen zur Hydrodynamik und Aerodynamik. Göttingen, 1927.
3. Smithsonian Mathematical Formulae and Tables of Elliptic Functions. Publication 2672, Smithsonian Institution, 1922.

TABLE I

VALUES OF  $\sinh \pi r$ ,  $\cosh \pi r$  AND  $\delta$ 

$$\delta_1 = \frac{\pi}{4} r \left( \sum_1^p \frac{\cosh n\pi r}{\sinh^2 n\pi r} + \frac{1}{12} \right) + \frac{1}{4 \sinh \left( p + \frac{1}{2} \right) \pi r} \text{ closed tunnel}$$

$$\delta_2 = \frac{\pi}{4} r \left( \sum_1^\infty \frac{(-1)^n}{\sinh^2 n\pi r} - \frac{1}{6} \right) \text{ free jet}$$

$$\delta_3 = \frac{\pi}{4} r \left( \sum_1^\infty \frac{(-1)^n \cosh n\pi r}{\sinh^2 n\pi r} + \frac{1}{12} \right) \text{ horizontal boundaries}$$

$$\delta_4 = \frac{\pi}{4} r \left( \sum_1^p \frac{1}{\sinh^2 n\pi r} - \frac{1}{6} \right) + \frac{1}{4} \coth \left( p + \frac{1}{2} \right) \pi r \text{ vertical boundaries}$$

$$\delta_5 = \frac{\pi}{4} \frac{r}{2} \left( \sum_1^\infty \frac{(-1)^n \cosh \frac{n\pi r}{2}}{\sinh \frac{n\pi r}{2}} + \frac{1}{12} \right) \text{ one horizontal boundary}$$

$r$	$\sinh \pi r$	$\cosh \pi r$	$r$	$\delta_1$	$\delta_2$	$\delta_3$	$\delta_4$	$\delta_5$
0	0	1.00	0	$\infty$	$-\infty$	$-\infty$	$+\infty$	$-\infty$
.125	.4032	1.078	.125	1.055	-0.524	-0.524	+1.051	-1.050
.250	.8686	1.324	.25	.523	-.262	-.262	+.524	-.524
.375	1.4702	1.778	.50	.263	-.137	-.127	+.262	-.262
.500	2.299	2.507	.625	.213	-.122	-.089	+.210	-.208
.625	3.492	3.632	.75	.175	-.120	-.056	+.161	-.173
.750	5.227	5.322	1.00	.138	-.137	.000	+.124	-.127
1.00	11.530	11.574	1.50	.120	-.197	+.077	+.054	-.056
1.50	55.52	55.53	2.00	.137	-.262	+.126	-.012	.000
2.0	267	267	4.00	.262	-.524	+.262	-.276	.126
$\infty$	$\infty$	$\infty$	$\infty$	$\infty$	$-\infty$	$+\infty$	$-\infty$	$+\infty$